Quantifying mixing in arbitrary fluid domains: A Padé approximation approach

Thomas G. Anderson[*], Marc Bonnet[†], and Shravan Veerapaneni[*‡]

Abstract

We consider the model problem of mixing of passive tracers by an incompressible viscous fluid. Addressing questions of optimal control in realistic geometric settings or alternatively the design of fluid-confining geometries that successfully effect mixing requires a meaningful norm in which to quantify mixing that is also suitable for easy and efficient computation (as is needed e.g. for use in gradient-based optimization methods). We use the physically-inspired reasonable surrogate of a negative index Sobolev norm over the complex fluid mixing domain Ω, a task which could be seen as computationally expensive since it requires the computation of an eigenbasis for $L^2(\Omega)$ by definition. Instead, we compute a representant of the scalar concentration field in an appropriate Sobolev space in order to obtain an equivalent definition of the Sobolev surrogate norm. The representant, in turn, can be computed to high-order accuracy by a Padé approximation to certain fractional pseudo-differential operators, which naturally leads to a sequence of elliptic problems with an inhomogeneity related to snapshots of the time-varying concentration field. Fast and accurate potential theoretic methods are used to efficiently solve these problems, with rapid per-snapshot mix-norm computation made possible by recent advances in numerical methods for volume potentials. We couple the methodology to existing solvers for Stokes and advection equations to obtain a unified framework for simulating and quantifying mixing in arbitrary fluid domains. We provide numerical results demonstrating the convergence of the new approach as the approximation order is increased.

Key words. mix norm, Stokes flow, integral equations, Padé approximation

1 Introduction

This article concerns fluid mixing processes, whereby some spatially-varying quantity, hereafter denoted by c and called concentration, is advected by fluid motion. An important objective, then, is to achieve optimal mixing whereby c becomes spatially near-uniform after sufficient time under appropriate advection. Pure advection in a fluid domain $\Omega \subset \mathbb{R}^d$ is modeled by the partial differential equation (PDE) for the function $c = c(\boldsymbol{x}, t)$

$$\partial_t c + \boldsymbol{\nabla} c \cdot \boldsymbol{u} = 0 \quad \text{for} \quad (\boldsymbol{x}, t) \in \Omega \times [0, T], \tag{1}$$

which for a flow velocity field $\boldsymbol{u} = \boldsymbol{u}(\boldsymbol{x}, t)$ defined on $\Omega \times [0, T]$ and satisfying the incompressibility condition $\boldsymbol{\nabla} \cdot \boldsymbol{u} = 0$ expresses that the material derivative of c in the flow $\boldsymbol{u}$ vanishes or, equivalently, that c is conserved when following the material motion. For simplicity, we restrict attention here to viscous flows modeled by the Stokes equations, but the principal objectives and results translate to transport and mixing by more complex fluids; we also restrict attention in our numerical experiments to two-dimensional flows, $d = 2$, though the methodology applies seamlessly to the case $d = 3$. It is important to quantify the departure of c from a spatially uniform distribution, for instance as a means

[*]Department of Mathematics, University of Michigan, Ann Arbor, MI, 48109 USA
[†]POEMS (CNRS, INRIA, ENSTA), ENSTA Paris, 91120 Palaiseau, France
[‡]Corresponding author, *email:* shravan@umich.edu

to design stirring flow motions that promote even mixing. Once a mixing measure has been established a variety of questions concerning optimal mixing, including under constraints on either some appropriate norm of the flow velocity itself or instead potentially forcing to effect such a flow (such as e.g. fixed energy or power), can be considered [1, 2]. While it appears natural to measure the unevenness of (i.e. relative to its mean value $\overline{c}(t)$) in terms of its L^2 variance,

$$\mathrm{Var}[c](t) := \|c(\cdot,t)-\overline{c}(t)\|^2_{L^2(\Omega)} \quad \text{with} \quad \overline{c}(t) = |\Omega|^{-1}\big(c(\cdot,t),1\big)_{L^2(\Omega)},$$

where $\big(\cdot,\cdot\big)_{L^2(\Omega)}$ and $\|\cdot\|_{L^2(\Omega)}$ denote, respectively, the inner product and induced norm on $L^2(\Omega)$, the quantity $\mathrm{Var}[c](t)$ unfortunately turns out to be conserved in time, $\mathrm{dVar}[c](t)/\mathrm{d}t = 0$, for the simple situation of pure (diffusionless) advection of c by incompressible flows[1].

This has elicited the definition of alternative methods for measuring mixing quality, notably the concept of mix-norm [4, 3]. The (squared) mix-norm $\Phi(c)$ of a concentration c is defined as a quadratic mean of the concentration averages evaluated on all balls with centers and radii compatible with the given fluid domain Ω. Evenness of mixing is then measured in terms of (reducing) the mix-variance $\Phi\big(c-\overline{c}\big)$. The mix-norm $\Phi(c)$ of c can be formulated analytically (using Fourier series) for periodic domains (where Ω is the periodic cell such that the intersection of balls with radii of all sizes with centers near $\partial\Omega$ are well-defined, and where the fluid velocity $\boldsymbol{u}$ is also Ω-periodic). On the other hand, the construction method of the mix-norm makes its evaluation impractical and inefficient for flows in arbitrary bounded fluid domains Ω.

In light of this difficulty, it is fortunate that the mix-norm $\Phi(c)$ for periodic mixing has been shown [4] to be equivalent to the $H^{-1/2}(\Omega)$ Sobolev norm of c. More generally [1], weighted versions of $\Phi(c)$ are equivalent to $H^{-r}(\Omega)$ Sobolev norms with $1/2 \le r \le 1$ (the value of r depending on the chosen weight); for example, the mixing enhancement study [5] uses $r = 2/3$, wherein a low-order penalization technique was used to reduce the problem to a periodic setting. As Sobolev norms can *a priori* be defined for functions in arbitrary fluid domains, the foregoing norm equivalence results for periodic flows lead naturally to the idea of using Sobolev norms with appropriate negative indices as mix-norm surrogates that, unlike the original mix-norm, are applicable for arbitrary flow configurations.

This work accordingly rests on the premise that mixing by a flow in an arbitrary fluid domain Ω can adequately be measured by means of the variance $\Phi^2_r(c) := \|c-\overline{c}\|^2_{H^{-r}(\Omega)}$ associated with the Sobolev norm $\|\cdot\|^2_{H^{-r}(\Omega)}$ with negative index $-r$. We focus on the range $1/2 \le r \le 1$ of main practical interest, our approach being also valid for $0 \le r < 1/2$ (Remark 5). In this framework, our main objective is to formulate and demonstrate computational methods for the practical evaluation of $\Phi^2_r(c)$. Indeed, as discussed later in more detail, this task is far from straightforward due to the lack of explicit expressions of negative Sobolev norms of a given function c in Ω. One approach, which constitutes an extension of the Fourier series formulation for periodic flows, consists in expanding c in terms of the Laplace Dirichlet eigenfunctions φ_n ($n \in \mathbb{N}$) for Ω and evaluating $\Phi^2_r(c)$ as a sum of appropriately weighted squares of expansion coefficients (see Sec. 2.2 for details). This treatment is computationally expensive, since it entails first the computation of accurate approximations of φ_n to sufficiently high order, then expensive numerical quadrature for the precise evaluation of the projections $\big(c,\varphi_n\big)$ of c on the increasingly-oscillatory eigenfunctions. In view of this, and taking some inspiration from the boundary element literature where approximations of fractional Sobolev norms or fractional pseudo-differential operators on surfaces are used for error estimation or preconditioning [6], we propose in this work to use a formulation of $\Phi^2_r(c)$ in terms of the Riesz representant $u[c]$ of c in $H^r(\Omega)$ and compute an approximation of $u[c]$ using a Padé approximant of the operator $(I-\Delta)^r$, where Δ denotes the Dirichlet Laplacian operator on Ω. This results in $\Phi^2_r(c)$ being evaluated by combining the solutions of elliptic problems on Ω arising from the Padé approximation process, the number of which scaling proportionally with the desired Padé approximation order and being in practice moderate. Also, any linear elliptic solver may be used for this purpose, the numerical results presented in this work being obtained with boundary integral equation methods. The eigenfunction and Padé approaches are in fact linked (see Section 3.2). We finally mention that the Dunford-Taylor integral representation of fractional operators leads to similar numerical solution strategies for $u[c]$ [7, 8] (also, see Remark 4).

[1]Note that even in the presence of diffusion (with diffusion constant, $\kappa > 0$) it is worthwhile to consider alternative metrics of mixing, since the limit $\kappa \to 0$ is singular in a way that impacts mixing studies; see, e.g. [3] for a detailed discussion.

The main advantages of our approach compared to existing eigenfunction approaches can be summarized as follows. Firstly, evaluating Dirichlet eigenfunctions on complex domains is a computationally challenging problem: even recently proposed methods [9] still carry significant costs for computation for a set of high-frequency eigenfunctions—the cost growing polynomially with the size of the desired eigenbasis. Secondly, accurate projection onto these high-frequency eigenfunctions may require an unnecessarily fine spatial resolution in the underlying fluid solver. In contrast, the solution of sign-definite elliptic problems is a long-studied problem with well-known optimal complexity acceleration algorithms, e.g. multigrid and fast multipole methods (FMMs) [10]; we rely on FMMs in conjunction with recently-developed volume solvers to solve each elliptic problem in linear time.

The organization of this article is as follows. The proposed Riesz-representant approach to the evaluation of $\Phi_r^2(c)$ is presented in Section 2, together with a concise summary of the underlying Sobolev framework and the eigenfunction-based norm evaluation used here for comparison purposes. The proposed Padé approximation approach to $\Phi_r^2(c)$ is then given in Section 3, and assessed in Section 4 on numerical experiments involving norm evaluation and mixing by Stokes flows.

2 Sobolev mix-norm and its practical computation

Our main objective is to develop practical methods for the evaluation of the surrogate mix-variance

$$\Phi_r^2(c) := \|c - \overline{c}\|_{H^{-r}(\Omega)}^2, \tag{2}$$

defined in terms of the Sobolev norm $\|\cdot\|_{H^{-r}(\Omega)}^2$ with negative index $-r$ $(1/2 \le r \le 1)$, on a given snapshot of the concentration c in the fluid domain Ω. To evaluate $\Phi_r^2(c)$ as a function of time in an advection process (1), definition (2) is applied at each time t to $c(\cdot, t)$ in Eulerian representation.

2.1 Sobolev norms with fractional indices: an overview

We begin by collecting known definitions and facts about Sobolev norms with fractional indices; for a concise yet quite informative exposition on Sobolev spaces, see [11, Chap. 2]. First considering functions or distributions whose support is $\mathbb{R}^d$, the Sobolev space $H^r(\mathbb{R}^d)$ may be defined, for any index $r \in \mathbb{R}$, in terms of the Fourier-Bessel scalar product and norm:

$$(v, w)_{r,\mathbb{R}^d} := \big(\boldsymbol{\xi} \mapsto (|\boldsymbol{\xi}|^2+1)^{r/2}\hat{v}(\boldsymbol{\xi}), \boldsymbol{\xi} \mapsto (|\boldsymbol{\xi}|^2+1)^{r/2}\overline{\hat{w}(\boldsymbol{\xi})}\big)_{L^2(\mathbb{R}^d)}, \qquad \|v\|_{r,\mathbb{R}^d}^2 := (v, v)_{r,\mathbb{R}^d}, \tag{3}$$

where $\hat{v} : \mathbb{R}^d \to \mathbb{C}$, is the Fourier transform of v and $\boldsymbol{\xi} \in \mathbb{R}^d$ is the generic vector in Fourier space. Noting that $|\boldsymbol{\xi}|^2$ is the Fourier symbol of $-\Delta$, we observe that the $H^r(\mathbb{R}^d)$ norm (3) can be expressed using Plancherel's theorem, as

$$\|v\|_{r,\mathbb{R}^d} := \big\|(I-\Delta)^{r/2} v\big\|_{L^2(\mathbb{R}^d)}$$

in terms of a fractional power $(I-\Delta)^\alpha$ of the elliptic operator $I-\Delta$ on $\mathbb{R}^d$ defined by

$$\mathcal{F}\big[(I-\Delta)^\alpha v\big](\boldsymbol{\xi}) = (1+|\boldsymbol{\xi}|^2)^\alpha \hat{v}(\boldsymbol{\xi}).$$

Analogous definitions are available for spatially periodic functions, based on Fourier series expansions instead of the Fourier transform.

In this work, we focus on (negative fractional) Sobolev norms of functions defined in a given bounded domain $\Omega \subset \mathbb{R}^d$, and notations $(\cdot,\cdot)_r$ or $\|\cdot\|_r$ implicitly refer to that domain. For this case, the Fourier-Bessel framework provides

$$\|v\|_r = \min_{V \in H^r(\mathbb{R}^d),\, V|_\Omega = v} \|V\|_{r,\mathbb{R}^d},$$

which is not well suited to the practical evaluation of $\|v\|_{r,\Omega}$. Alternatively, for positive fractional indices $r \in (0,1)$,

$$\|v\|_r^2 := \|v\|_0^2 + \int_\Omega \int_\Omega \frac{(v(\boldsymbol{y}) - v(\boldsymbol{x}))^2}{|\boldsymbol{y}-\boldsymbol{x}|^{d+2r}} \,\mathrm{d}V(\boldsymbol{x})\,\mathrm{d}V(\boldsymbol{y}) \tag{4}$$

defines a norm for $H^r(\Omega)$; the double-integral term is known as the Slobodeckij semi-norm. Formula (4) is explicit, but evaluating the semi-norm is potentially expensive (due to the $2d$-dimensional integral over $\Omega\times\Omega$) and requires suitable quadrature methods since a (weakly) singular integral is involved. Another possibility consists in setting again

$$\|v\|_r := \big\|(I-\Delta)^{r/2}v\big\|_0 \tag{5}$$

with fractional operators $(I-\Delta)^\alpha$ on Ω now defined from the spectral decomposition of the Laplacian on Ω (see Section 2.2).

For negative indices, our primary concern, explicit formulas for $H^{-r}(\Omega)$ norms are not available for arbitrary domains. In fact, elements of $H^{-r}(\Omega)$ are, by the definition of that space, continuous linear functionals on $\widetilde{H}^r(\Omega) := \big\{v|_\Omega \,:\, v\in H^r(\mathbb{R}^d),\ \mathrm{supp}(v)\subset\overline{\Omega}\big\}$, and their norm is therefore defined by duality. By Riesz's representation theorem, there exists a unique function $u[c]\in\widetilde{H}^r(\Omega)$ such that

$$\big(u[c],v\big)_r = \big\langle c,v\big\rangle \qquad \text{for all } v\in\widetilde{H}^r(\Omega), \tag{6}$$

(the duality bracket $\big\langle c,v\big\rangle$ denoting $c\in H^{-r}(\Omega)$ evaluated at $v\in\widetilde{H}^r(\Omega)$, with $\big\langle c,v\big\rangle=(c,v)_0$ under the present assumption that $c\in L^2(\Omega)$), which for $r>\frac12$ can be understood as the weak form of the problem

$$(I-\Delta)^r u[c]=c, \qquad \gamma u[c]=0$$

(where γw denotes the boundary trace of $w\in H^r(\Omega)$). Moreover, $u[c]$ satisfies

$$\|c\|_{-r}=\|u[c]\|_r. \tag{7}$$

Then, by (7), we have

$$\|c\|_{-r}^2=\|u[c]\|_r^2=\big\langle u[c],c\big\rangle=\big(u[c],c\big)_0 \tag{8}$$

(since, again, $c\in L^2(\Omega)$ by assumption). If $r\in\,]\frac12,1[$ and Ω is a Lipschitz domain, we have $\widetilde{H}^r(\Omega)=H_0^r(\Omega)$, and all elements of $\widetilde{H}^r(\Omega)$ have a vanishing trace on $\partial\Omega$. A practical method for evaluating $\|c\|_{-r}$ thus consists in the following steps: (a) compute the Riesz representant $u[c]$ of c for the $H^{-r}(\Omega)$ norm by solving problem (6), and (b) evaluate $\|c\|_{-r}$ using (8). In (6), the $H^r(\Omega)$ scalar product and norm may be defined in terms of $(I-\Delta)^r$ where Δ is the Dirichlet Laplacian on Ω.

Remark 1 (special case $r=1$) *For $r=1$, the H^1 norm is simply given by $\|v\|_1^2=\|v\|_0^2+\|\boldsymbol{\nabla}v\|_0^2$, and $\|v\|_{H_0^1(\Omega)}^2:=\|\boldsymbol{\nabla}v\|_0^2$ defines an equivalent norm for $H_0^1(\Omega)$. In particular, by contrast with the fractional-index case, those norms are additive with respect to partitions of Ω (e.g. finite elements). Problem (6) becomes the weak form of the Poisson equation with homogeneous Dirichlet condition and domain source term c, a problem easily solvable using a variety of standard numerical methods. Then, $\|c\|_{-1}^2=\big(\boldsymbol{\nabla}u[c],\boldsymbol{\nabla}u[c]\big)_0$.*

Remark 2 (link to Sobolev interpolation) *The norm (5) with Δ the Dirichlet Laplacian on Ω is suitable for equipping the interpolation space $\big[H_0^1(\Omega),L^2(\Omega)\big]_{1-r}$. For $r\in\,]\frac12,1[$, we have $\big[H_0^1(\Omega),L^2(\Omega)\big]_{1-r}=H_0^r(\Omega)$. For $r=\frac12$, we have $\big[H_0^1(\Omega),L^2(\Omega)\big]_{1-r}=H_{00}^r(\Omega)$, with $H_{00}^r(\Omega)$ strictly contained in $H_0^r(\Omega)$ and having a strictly finer topology, see [12, Chap. 1]. Problem (6) thus defines the Riesz representant of an element of $(H_0^r(\Omega))'=H^{-r}(\Omega)$ if $r\in\,]\frac12,1[$, and of an element of $(H_{00}^r(\Omega))'$ if $r=\frac12$*

2.2 Evaluation using a Hilbert basis

This section describes the computation of $\|c\|_{-r}$ using the spectral decomposition of the Dirichlet Laplacian and the associated $L^2(\Omega)$-orthonormal Hilbert basis. Let $(\varphi_n)_{n\geq0}$ be a countable set of Laplacian eigenfunctions for Ω, which satisfy $-\Delta\varphi_n=\lambda_n\varphi_n$ in Ω and $\gamma\varphi_n=0$, the eigenvalues λ_n being strictly positive. Normalizing the φ_n so that $\|\varphi_n\|_0=1$, we also have $\|\boldsymbol{\nabla}\varphi_n\|_0^2=\lambda_n$. The set $(\varphi_n)_{n\geq0}$ is a Hilbert basis of $L^2(\Omega)$, while $\lambda_n^{-1/2}(\varphi_n)_{n\geq0}$ defines a Hilbert basis of $H_0^1(\Omega)$.

For $c = \sum_{n\geq 0} c_n\varphi_n$ in $L^2(\Omega)$ (so that $c_n = (c,\varphi_n)_0$), we may define the evaluation of the operator $f(\Delta)$ on c by

$$f(\Delta)c = \sum_{n\geq 0} f(-\lambda_n)c_n\varphi_n \tag{9}$$

whenever the sequence $|f(-\lambda_n)c_n|^2$ is summable (this criterion defining the domain of $f(\Delta)$ on $L^2(\Omega)$). In particular, the summability requirement is satisfied with $f(X) = (1-X)^{-r}$ for any $r \geq 0$, and (9) allows to evaluate $(I-\Delta)^{-r}$ for any $r \in (0,1)$ [7]. The Riesz representant $u[c]$ of c is then obtained as

$$u[c] = (I-\Delta)^{-r}c = \sum_{n\geq 0}(1+\lambda_n)^{-r}c_n\varphi_n$$

and (8) therefore yields

$$\|c\|_{-r}^2 = \sum_{n\geq 0}(1+\lambda_n)^{-r}c_n^2.$$

For $f(X) = (1-X)^{-r}$, this procedure evaluates $u[c]$ as an element of the interpolation space $\left[H_0^1(\Omega), L^2(\Omega)\right]_{1-r}$, see Remark 2.

3 Negative Sobolev norm evaluation using Padé approximants

While the Hilbert basis approach to mix-norm evaluation allows in principle the numerical evaluation of $\|c\|_{-r}$ in general geometries, it is prohibitively expensive as it relies on production of an appropriate set of oscillatory eigenfunctions (itself a challenging computational problem) onto which the scalar fields must be accurately projected. In this section we first outline a practical, computationally-efficient approach based on Padé approximation [13] and then connect this approach back to the Hilbert basis evaluation described in Section 2.2.

3.1 Practical method

To avoid reliance upon a (truncated) set of eigenfunctions, computable approximations of the operator $(I-\Delta)^{-r}$ (and, more generally, of operators of the form $f(\Delta)$, where Δ is the Dirichlet Laplacian) can be set up using Padé approximations [14] of the function $f(X) = (1-X)^{-r}$.

A Padé approximant of a univariate function $f(X)$ is a rational fraction $\Pi_{m,n}[f](X) := P_m(X)/Q_n(X)$ (where P and Q are polynomials of respective degrees m and n) such that the $m+n$ degree Taylor polynomials of f and $\Pi_{m,n}[f]$ about $X=0$ coincide (i.e. the Taylor expansion of $f-\Pi_{m,n}[f]$ is $0+o(X^{m+n})$). There is naturally some flexibility in how to choose the degrees m and n; here we make the selection $m=n-1$, i.e. we use Padé approximants $\Pi_n[f] := \Pi_{n-1,n}[f]$ (see also Remark 3). A classical method for computing the coefficients of the polynomials P_{n-1}, Q_n is summarized in Appendix B. The next step consists in recasting $\Pi_n[f]$ as a partial fraction decomposition: we have

$$\Pi_n[f](X) = \sum_{k=1}^{n} \frac{A_n^k}{X_n^k - X} \quad \text{with} \quad A_n^k = -\frac{P_{n-1}(X_n^k)}{Q_n'(X_n^k)} \tag{10}$$

where $X_n^1, \ldots, X_n^n$ are the roots of Q_n, which are assumed to be distinct (i.e. of unit multiplicity). If each of the roots X_n^k is positive (which is for example the case for $f(X) = (1-X)^{-1/2}$, i.e. $r = \frac{1}{2}$), then each of the operators $X_n^k - \Delta$ is elliptic. The approximation of $u[c] = f(\Delta)c$ solving problem (6) provided for a given concentration c by the Padé approximant (10) is then

$$u[c] \approx \sum_{k=1}^{n} A_n^k w_k \qquad \text{where } w_k \text{ solves} \quad (X_n^k - \Delta)w_k = c \text{ in } \Omega,\ \gamma w = 0 \text{ on } \partial\Omega. \tag{11}$$

To define the w_k uniquely in (11), boundary conditions must be specified. Indeed, notice that for positive r the function $(I-\Delta)^{-r}v$ is in some sense an antiderivative of v, which is not uniquely defined unless additional conditions (such as boundary conditions on w_k) are supplied.

n	avg. λ	max. λ	n	avg. λ	max. λ
3	2.1	3.9	19	3.3	24.2
4	2.3	5.1	21	3.3	26.7
5	2.4	6.4	23	3.4	29.3
6	2.5	7.7	25	3.5	31.8
7	2.6	8.9	27	3.5	34.4
8	2.7	10.2	31	3.6	39.5
9	2.8	11.5	35	3.7	44.6
11	2.9	14.0	39	3.7	49.7
13	3.0	16.6	43	3.8	54.8
15	3.1	19.1	47	3.9	59.8
17	3.2	21.7	51	3.9	64.9

Table 1: *Statistics of the Helmholtz parameter $\lambda = \sqrt{X_n^k}$ that arise for the Padé approximants of the indicated order. For odd n, the median λ value is always $\lambda = \sqrt{2}$, as indeed in this case $X_n^k = 2$ is always a root of Q_n. Put another way, for each n, at least half of all required modified Helmholtz problems are of approximately equal (and minimal) cost even as the maximum λ increases. Similar behavior is observed for other values of r.*

Remark 3 *The specific degrees of polynomials used in our Padé approximants are somewhat arbitrary; the Padé approximants $\Pi_n[f] = \Pi_{n-1,n}[f]$ used here generate partial fraction approximations without a constant term, but other choices appear equally valid. Variations may also be considered for the choice of fractional operator; for example, replacing the operator $(1-\Delta)^{-r}$ that we treat here with $(1-\mu^{-1}\Delta)^{-r}$, where μ is an estimate of the first (lowest) Dirichlet eigenvalue $\lambda_1(\Omega)$ for the domain Ω, removes length scale effects in that operator. Such estimates can be obtained e.g. from the Faber-Krahn inequality that provides $\lambda_1(\Omega) \geq \mu$ with $\mu = \pi z_{0,1}^2/|\Omega|$ ($d = 2$, with $z_{0,1}$ as in Appendix A) or $\mu = (4\pi^4/3|\Omega|)^{2/3}$ ($d = 3$).*

Remark 4 *Alternative numerical approximation methods for the evaluation of fractional elliptic operators are developed and justified in [7, 8] on the basis of Dunford-Taylor integral representations of such operators. In the case of $(I-\Delta)^{-r}$, we have [7]*

$$(I-\Delta)^{-r}c = \frac{2\sin(\pi r)}{\pi}\int_0^\infty t^{2r-1}(I-t^2\Delta)^{-1}c\,dt$$

for any $c \in L^2(\Omega)$, where $(I-t^2\Delta)^{-1}c = u_t[c]$ solves the variational elliptic problem: find $u_t[c] \in H_0^1(\Omega)$ such that $(u,w)_0 + t^2(\boldsymbol{\nabla} u[c], \boldsymbol{\nabla} w)_0 = c$ for all $w \in H_0^1(\Omega)$. Upon applying a quadrature rule (involving finitely many nodes and weights) to the above integral, one has to evaluate a finite linear combination of solutions of elliptic problems, similarly to the proposed Padé approximation approach.

Remark 5 *Although we focus in this work on the cases $1/2 \leq r \leq 1$, the proposed Padé-based treatment also applies to the cases $0 \leq r < 1/2$, for which $H^r(\Omega) = H_0^r(\Omega) = \widetilde{H}_0^r(\Omega)$ (any element of $\widetilde{H}_0^r(\Omega)$ thus being the limit of some sequence of functions with vanishing Dirichlet trace).*

3.2 Link between Padé approximations and eigenfunction expansions

For the purposes of comparison, it is useful to reformulate the Padé approximation approach of Sec. 3 by means of the Hilbert basis of Laplacian eigenfunctions introduced in Sec. 2.2. Letting $v = \sum_{m\geq 0} v_m\varphi_m$ and $w_k = \sum_{m\geq 0} w_m^k\varphi_m$, the problem $(X_n^k - \Delta)w_k = v$ with homogeneous Dirichlet BCs becomes

$$\sum_{m\geq 0}(X_n^k+\lambda_m)w_m^k\varphi_m = \sum_{m\geq 0} v_m\varphi_m \quad \Longrightarrow \quad w_m^k = \frac{v_m}{X_n^k+\lambda_m}.$$

The Padé approximation (11) of $f(\Delta)v$, found to be given by

$$f(\Delta)v \approx \sum_{k=1}^n A_n^k\Big(\sum_{m\geq 0}\frac{v_m}{X_n^k+\lambda_m}\varphi_m\Big) = \sum_{m\geq 0}\Big(\sum_{k=1}^n \frac{A_n^k}{X_n^k+\lambda_m}\Big)v_m\varphi_m = \sum_{m\geq 0}\Pi_n[f](-\lambda_m)v_m\varphi_m, \quad (12)$$

is formula (9) with $f(-\lambda_m)$ replaced with its Padé approximation $\Pi_n[f](-\lambda_m)$. This indicates consistency between the eigenfunction-expansion and Padé-approximation treatments. It also allows an understanding of the effectiveness of the numerical approximation (12) to $f(\Delta)v$ via knowledge of the approximating power for the scalar problem for $\Pi_n[f](X)$.

3.3 Numerical methods and algorithms

This section describes the mathematical and computational framework used in the experiments of the present work. We first briefly outline relevant aspects of the conservation law package used for solving (1), then describe the use of potential-theoretic techniques to solve the required elliptic problems for the Padé approximation to the mix-norm in (11), and finally describe standard boundary-integral solution techniques for the inhomogeneous Stokes equations to produce the flow field $\boldsymbol{u}$.

Concentration field evolution solver. The hyperbolic PDE (1) with no-outflow boundary conditions is solved using the `Clawpack v5.8.2` library [15, 16]; we refer the reader to reference [17] for a complete mathematical description of the finite volume solvers used in this software but we note that the solver computes solutions in logically-rectangular coordinates and provides automatic time-step selection as dictated by the physics of the system. The `Clawpack` description of fluid domains as a union of rectangular domains with explicitly known domain mappings constrains the complexity of geometry that we consider in this work; additionally, the solvers appear to be limited by a choice of low-order accuracy or uniform discretizations. While for the present purposes `Clawpack` allows a demonstration of the main capabilities of Padé-based approximations of the mix-norm for real-world mixing problems, future work will utilize more recently-developed high-order and adaptive hyperbolic conservation law solvers such as [18].

Elliptic problems for Padé approximants. The inhomogeneous elliptic PDE (11) is of modified Helmholtz type,

$$\begin{aligned} -\Delta v + \lambda v &= f \quad \text{for} \quad \boldsymbol{x} \in \Omega, \\ v &= 0 \quad \text{for} \quad \boldsymbol{x} \in \partial\Omega. \end{aligned} \tag{13}$$

A homogeneous counterpart to (13) can be obtained by linearity and the use of a particular solution v_P produced by the Newton potential

$$v_P(\boldsymbol{x}) := \int_\Omega G(\boldsymbol{x}, \boldsymbol{y}) f(\boldsymbol{y}) \, \mathrm{d}V(\boldsymbol{y}), \quad \boldsymbol{x} \in \Omega, \tag{14}$$

where G denotes the Green function for the elliptic operator in (13). We solve this homogeneous elliptic problem, in turn, by introducing a representation of its solution in terms of the double-layer potential

$$\mathcal{D}[\psi](\boldsymbol{x}) := \int_{\partial\Omega} \frac{\partial G(\boldsymbol{x}, \boldsymbol{y})}{\partial \boldsymbol{n}(\boldsymbol{y})} \psi(\boldsymbol{y}) \, \mathrm{d}\sigma(\boldsymbol{y}), \quad \boldsymbol{x} \in \Omega. \tag{15}$$

That is, we set $v(\boldsymbol{x}) = v_P(\boldsymbol{x}) + \mathcal{D}[\psi](\boldsymbol{x})$. Enforcing the Dirichlet boundary condition and using jump relations for the double-layer potential [19] yields the following second-kind integral equation for the unknown density function ψ:

$$\left(\pm \frac{1}{2} I + D \right) [\psi](\boldsymbol{x}) = -v_P, \quad \boldsymbol{x} \in \Gamma_\pm. \tag{16}$$

Here, Γ_+ (resp. Γ_-) denotes that section of the boundary $\partial\Omega$ with respect to which the domain lays interior (exterior), and D denotes the double-layer boundary integral operator

$$D[\psi](\boldsymbol{x}) := \int_{\partial\Omega} \frac{\partial G(\boldsymbol{x}, \boldsymbol{y})}{\partial \boldsymbol{n}(\boldsymbol{y})} \psi(\boldsymbol{y}) \, \mathrm{d}\sigma(\boldsymbol{y}), \quad \boldsymbol{x} \in \partial\Omega.$$

We use standard spectral singular quadratures [19, §12] for discretization of the integral equation (16), spectral near-singular quadratures [20] for evaluation of the double layer potential (15) for $\boldsymbol{x}$ laying

in close proximity to $\partial\Omega$, and recently-introduced high-order accurate numerical methods [21] for the evaluation of the volume potential (14). Importantly in the present context where the spatial field c changes at every time-step, the solvers developed in [21] provide exceptionally-fast access to the volume potential over the same domain with new volumetrically-distributed sources.

Stokes problems for fluid velocity. The Stokes problem refers to the task of finding a velocity function $\boldsymbol{u}(\boldsymbol{x})$ and pressure function $p(\boldsymbol{x})$ that satisfy the PDE boundary value problem

$$\begin{aligned} -\mu\nabla^2\boldsymbol{u} + \nabla p = 0, &\quad \boldsymbol{x} \in \Omega \\ \nabla \cdot \boldsymbol{u} = 0, &\quad \boldsymbol{x} \in \Omega, \\ \boldsymbol{u} = \boldsymbol{g}(\boldsymbol{x}), &\quad \boldsymbol{x} \in \Gamma = \partial\Omega. \end{aligned} \tag{17}$$

where μ is the fluid viscosity. Analogous integral equations to those arising from the modified Helmholtz equation follow from use of the representation formula

$$\boldsymbol{u}(\boldsymbol{x}) = \boldsymbol{\mathcal{D}}[\boldsymbol{\varphi}](\boldsymbol{x}) := \int_{\partial\Omega} \frac{\partial \boldsymbol{G}_s(\boldsymbol{x},\boldsymbol{y})}{\partial \boldsymbol{n}(\boldsymbol{y})} \boldsymbol{\varphi}(\boldsymbol{y})\, \mathrm{d}\sigma(\boldsymbol{y}) \tag{18}$$

that yields a solution $\boldsymbol{u}$ induced by the boundary integral density $\boldsymbol{\varphi}$, where

$$\boldsymbol{G}_s(\boldsymbol{x},\boldsymbol{y}) = \frac{1}{4\pi\mu}\left(-\log|\boldsymbol{x}-\boldsymbol{y}|\boldsymbol{I} + \frac{(\boldsymbol{x}-\boldsymbol{y})\otimes(\boldsymbol{x}-\boldsymbol{y})}{|\boldsymbol{x}-\boldsymbol{y}|^2}\right)$$

is the free-space Green's function for the Stokes equations [22]. The resulting integral equations are again of Fredholm type of the second kind. As before, spectral quadratures are used in the discretization of the resulting integral equation that φ must solve for $\boldsymbol{u}$ to satisfy the boundary condition in (17).

The overall procedure that we have described in this paper to quantify fluid mixing is as follows. First, the Stokes boundary value problem (17) is solved using boundary integral equations and the velocity function $\boldsymbol{u}$ is accessible throughout the fluid domain Ω by means of (18). Using this velocity, a given initial concentration field $c = c(\boldsymbol{x}, t)$ is advected in accordance with the appropriate transport model (here following equation (1)) by means of the conservation law solver. At a desired snapshot in time t the mix-norm surrogate $\|c\|_{-r}$ is produced by first obtaining the representant $u[c(\cdot, t)]$ using (11) and then the norm finally via (8). The representant $u[c]$ is obtained via solution of problems of the form (13) using boundary integral equations and volumetric Newton potentials—for a given fixed geometry we note that rapid repeated evaluation of the elliptic problems is possible so that mix-norm evaluation is inexpensive relative to the advection solver.

4 Numerical Results

This section demonstrates the approximation quality of the Padé approximants described in this article, and then demonstrates the use of the mix-norm surrogate to characterize mixing in fluid flow simulations.

4.1 Negative Sobolev index norm evaluation using Padé approximation

This validation experiment concerns the computation of the mix-norm $\|\cdot\|_{H^{-r}(\Omega)}$, $r = \frac{1}{2}$, over the disc domain $B(0,1)$, using the Padé approximation method described in Sec. 3, with results referring to the left-hand panel of Figure 1 (the 'Padé' labels refer to computation of this norm via the representation (8)); comparisons are made to the reference evaluation of the same norm using a Hilbert basis for $L^2(\Omega)$ described in Section 2.2. This experiment considers the one-parameter family of $L^2(\Omega)$ functions on Ω defined by

$$c(\boldsymbol{x}) = \sin(\alpha\pi x_1)\sin(\alpha\pi x_2)(\rho - 1), \quad \rho = \left(x_1^2 + x_2^2\right)^{1/2}, \qquad \boldsymbol{x} = (x_1, x_2) \in \Omega,$$

which have an oscillatory character that varies with the parameter $\alpha \in \mathbb{R}$. The Hilbert basis, which is known analytically for this domain (see Appendix A), is truncated to $n < N$ and $m < M$ ($N = M = 20$)

and is used for computation both of the Fourier-based norm and the solution of the inhomogeneous modified Laplace problems (11); sufficient discretization of the fluid domain is used to ensure accurate projections onto this set of functions. This approximation suffices to represent both c and the associated Riesz representant $u[c]$ with a maximum error of 10^{-5} in Ω for the values of α considered in this experiment.

The right plot in Figure 1 shows the results of a similar experiment, this time for the annular domain $\Omega = B(0,1) \setminus \overline{B(0,\frac{1}{2})}$. For $\alpha \in \mathbb{R}$ we consider the computation of mix-norm of the concentration functions

$$c(\boldsymbol{x}) = \sin(\alpha\pi x_1)\sin(\alpha\pi x_2)(\rho - \tfrac{1}{2})(\rho - 1), \quad \rho = \left(x_1^2 + x_2^2\right)^{1/2} \qquad \boldsymbol{x} = (x_1, x_2) \in \Omega,$$

which are defined in Ω and satisfy $\gamma c = 0$. For this geometry it is still possible, though even here not completely computationally trivial, to obtain a basis of eigenfunctions (known analytically in terms of numerically-computed eigenvalues, see Appendix A). The Hilbert basis is truncated to $n < N$ and $m < M$ ($N = 35, M = 60$), and used to compute both the Fourier-based norm and the solution of the inhomogeneous modified Laplace problems in (11). This set of functions suffices to represent both c and the associated Riesz representant $u[c]$ with a maximum error of 10^{-4} in Ω for all values of α considered in this experiment. The ground truth for this experiment, labeled 'Fourier' in Figure 1, is again a mix-norm value obtained using a generalized Fourier series.

We draw a few conclusions from these experiments. First, it is evident from both experiments that convergence is rapid in Padé order (see also the right panel in Figure 3 for an explicit error-vs-order plot). We also note that as the value of the mix-norm decreases (as α increases in this experiment, and the input function c becomes more oscillatory) the accuracy of the numerical approximation to the norm decreases; that is, the norm approximation quality is not uniform across its range. This effect reflects the underlying approximation quality of Padé approximants to the function $(1 - X)^{-r}$, which are of highest quality for small values of X (corresponding to the first eigenvalues of the operator with less oscillatory associated eigenfunctions); indeed the accuracy of Padé-approximated mix-norms can be estimated via the approximation quality of the scalar problem. Studies with other values of the parameter r reveal similar accuracy levels with identical conclusions and are omitted.

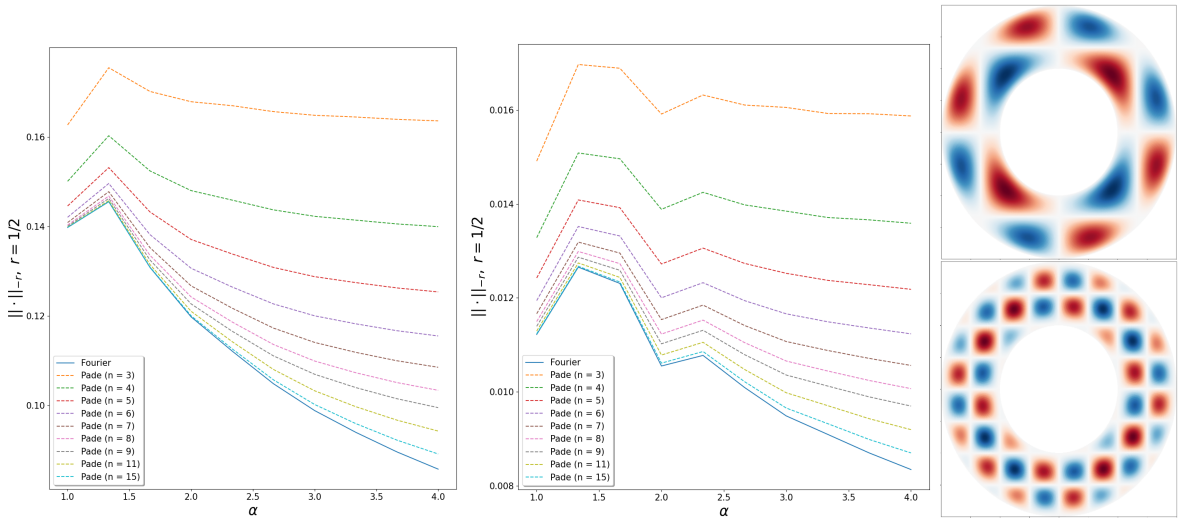

Figure 1: *Mix-norm $\|\cdot\|_{-r}$ with $r = \frac{1}{2}$. "Fourier" denotes the norm result when using the Hilbert basis of eigenfunctions, while the 'Padé' values correspond to the inner-product of the Riesz representant $u[c]$ in (8), and where the n value denotes the order of Padé approximation used in the computation of (11). Left: disc domain; Center: annular region; Right: concentration fields corresponding to $\alpha = 1.5$ (top) and $\alpha = 4.0$ (bottom) in the annular geometry.*

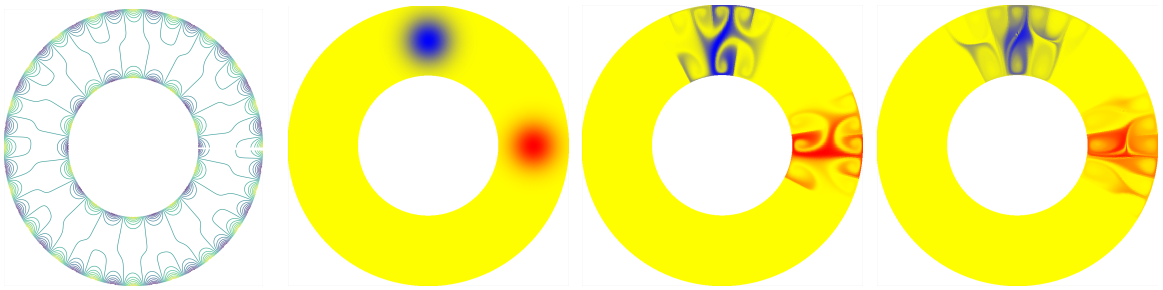

Figure 2: *Mixing in a narrow-channel Taylor-Couette device driven by a velocity field arising from a tangential slip boundary condition. Far-left: Vorticity of fluid flow induced by the tangential slip in the fluid mixing experiment. Left to Right: snapshots of concentration at* $t = 0$, $t = 1.0$, *and* $t = 3.0$.

4.2 Numerical demonstration of mix-norm application in incompressible flows

Here we consider mixing by a physically-realistic complex flow that arises as the solution to the Stokes equation with tangential slip boundary conditions (the flow is computationally found as the solution to a boundary integral formulation for the Stokes equations, cf. Section 3.3). The geometry is a Taylor-Couette device of inner radius $\rho_1 = 1/2$ and outer radius $\rho_2 = 1$, and is displayed in Figure 2. The initial scalar field consists of two Gaussian bump profiles, with opposing signs, namely,

$$c(\boldsymbol{x}) = e^{-40\left(x_1^2+(x_2-3/4)^2\right)} - e^{-40\left((x_1-3/4)^2+x_2^2\right)}, \quad \text{where} \quad \boldsymbol{x} = (x_1, x_2) \in \Omega.$$

We seek a velocity function $\boldsymbol{u}(\boldsymbol{x})$ and pressure function $p(\boldsymbol{x})$ that satisfy the Stokes boundary value problem (17) in this domain, wherein $\mathbf{g} = u_s\hat{\mathbf{t}}$ is a tangential slip boundary condition with $\hat{\mathbf{t}}$ the unit tangent vector on the positively-oriented boundary Γ. The prescribed slip magnitude u_s depends on the angular variable θ, and is given by $u_s(\theta) = \cos(\frac{m\ell}{2\pi}\theta)$, $m = 20$ (note that u_s is defined on both of the inner and outer circles of the annulus, and for each we take the parameter ℓ to equal the perimeter of that circle). The solution to the Stokes equations is computed to an accuracy level of approximately 10^{-8} as measured by self-convergence of the boundary integral equation solution with respect to the number of collocation nodes, while the conservation law solver, in turn, is discretized sufficiently to keep errors smaller than those observed in Figure 3.

To indicate the effectiveness of the proposed Padé approximation approach to the production of the mix-norm, we consider the convergence in Padé order for the mixing that results from this real flow (as before, the reference value of $\|c\|_{-1/2}$ is denoted by the 'Fourier' curves in Figure 3 and is obtained via a generalized Fourier series). Specifically, in Figure 3 we show convergence in the number n of Padé approximant terms for the Riesz representant $u[c]$ of c for the $H^{-r}(\Omega)$, $r = \frac{1}{2}$, norm. For each $0 \le k \le n$ we solve the elliptic problem in equation (11)), with absolute errors less than 10^{-5}, and proceed to compute the mix-norm $\|\cdot\|_{-r} = (u[c], c)_0$. The mixing can be seen in Figure 2, with relative errors at the final time $t = 2.5$ of 1.5% for $n = 14$ Padé approximant terms.

This experiment demonstrates the success of the mix-norm surrogate (8) as a means to quantify fluid mixing in arbitrary geometries. We note that the mixing displayed in the plots in Figure 2 with associated mix-norm evolution shown in the left-panel of Figure 3 captures even at very low Padé orders and relatively low accuracy the qualitative behavior of the mixing process. Furthermore, if high accuracy is desired, the right panel of Figure 3 demonstrates high-order convergence (in fact, near-exponential convergence with respect to the Padé approximant order n is apparent) to the true mix-norm surrogate, at the cost of an increasing number of elliptic solves. Similarly to the numerical results presented in the previous section, the plots in Figure 3 show a lack of uniform convergence, indicating a need for an increase in the Padé order for fixed relative error in the mix-norm value as mixing progresses, i.e. as the mix-norm is driven to zero.

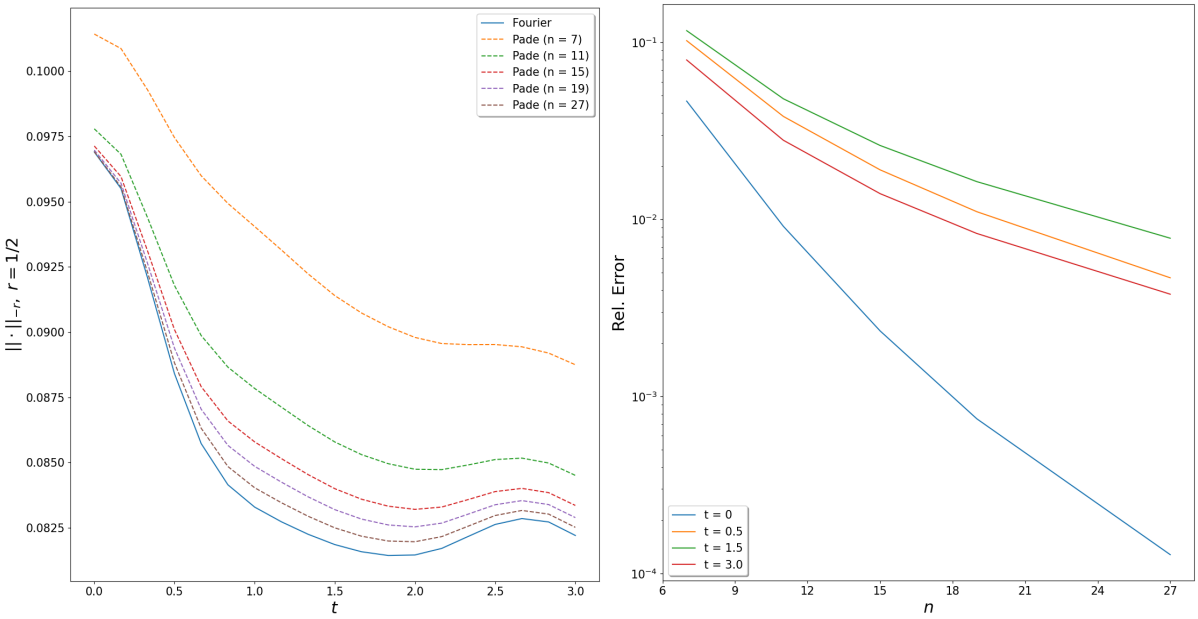

Figure 3: *Convergence in Padé order for the computation of the mix-norm in a setting of fluid mixing by a time-independent slip velocity.*

5 Conclusions

This work proposed and demonstrated the effectiveness of Padé approximants and the solution of certain associated elliptic PDEs to compute a mix-norm for tracers in incompressible flows that is both efficient in the presence of complex geometry and reduces the problem to well-understood problems in computational PDEs (inhomogeneous linear PDEs solved via volume potentials). This surrogate norm $\|\cdot\|_{-r}$ is equivalent to the Fourier based one but crucially avoids the need to compute eigenfunctions of the Laplacian over arbitrary domains. One weakness of the proposed Padé approximation strategy is the observed lack of uniformity in the error as the mix-norm decreases in value, which is the explicit goal of mixing studies; in ongoing work we seek to address this issue by developing alternate means to compute the Riesz representant associated with the surrogate mix-norm that both avoid this issue entirely and also require only a single inhomogeneous solve. The work could be straightforwardly extended to three dimensions, but requires efficient volume solvers for evaluation of (14) in that context, which is an area of active research. In contrast to the steady-state velocities considered here, time-varying velocities are of course not only possible (and expected, in order to achieve optimal mixing rates) to efficiently compute in the present context but will naturally be explored in future work in the context of optimal control.

A Eigenfunction expansion in circular or annular domains

Circular domain. Let $\Omega = B(0,a) = \{\boldsymbol{x}(\rho,\theta),\, 0 \le \rho < a,\, 0 \le \theta < 2\pi\}$ be the disk of radius a. The Dirichlet Laplace eigenfunctions for Ω are

$$\varphi_{0m} = \gamma_{0m} J_0(z_{0m}\rho/a), \quad \varphi^{(1)}_{nm} = \gamma_{nm} J_n(z_{nm}\rho/a)\cos n\theta, \quad \varphi^{(2)}_{mn} = \gamma_{nm} J_n(z_{nm}\rho/a)\sin n\theta \tag{19}$$

where J_n is the Bessel function of first kind and integer order n and z_{nm} $(m = 1, 2, \ldots)$ are the (real, positive) zeros of J_n (the excluded zero $z = 0$ of J_n $(n \ge 1)$ not producing nonzero eigenfunctions). Setting the normalization constants to $\gamma_{0m} = \sqrt{\pi}\big[aJ_1(z_{0m})\big]^{-1}$ and $\gamma_{nm} = \sqrt{\pi/2}\big[aJ_{n+1}(z_{nm})\big]^{-1}$ $(n \ge 1)$, the eigenfunctions (19) are $L^2(\Omega)$-orthonormal and satisfy

$$-\Delta\varphi_{0m} = \lambda_{0m}\varphi_{0m} \quad \text{and} \quad -\Delta\varphi^{(1,2)}_{nm} = \lambda_{nm}\varphi^{(1,2)}_{nm}, \qquad \text{with} \quad \lambda_{nm} = z^2_{nm}/a^2 \quad (n, m \ge 0).$$

As (Dirichlet) Laplace eigenfunctions, the functions (19) define a Hilbert basis of $L^2(\Omega)$, so that any $c \in L^2(\Omega)$ admits the expansion

$$c(\rho,\theta) = \sum_{m\geq 0}\Big\{ c_{0m}\varphi_{0m}(\rho,\theta) + \sum_{n\geq 1}\big(c^{(1)}_{nm}\varphi^{(1)}_{nm}(\rho,\theta) + c^{(2)}_{nm}\varphi^{(2)}_{nm}(\rho,\theta)\big)\Big\}$$

with $c_{0m} = \big(\varphi_{0m}, c\big)_{L^2(\Omega)}$ and $c^{(1,2)}_{nm} = \big(\varphi^{(1,2)}_{nm}, c\big)_{L^2(\Omega)}$. The $H^{-r}(\Omega)$ norm of c is therefore given by

$$\|c\|^2_{-r} = \sum_{m\geq 0}\Big\{ (1+\lambda_{0m})^{-r}[c_{0m}]^2 + \sum_{n\geq 1}(1+\lambda_{nm})^{-r}\big([c^{(1)}_{nm}]^2 + [c^{(2)}_{nm}]^2\big)\Big\}.$$

Annular domain. Let now $\Omega = B(0,\rho_1)\backslash\overline{B(0,\rho_2)}$ be the annulus of internal radius ρ_2 and external radius ρ_1. The (unnormalized) radial Dirichlet eigenfunctions for Ω are given by the expression

$$f_{nm}(\rho) = \frac{-1}{J_n(\zeta_{nm}\rho_1)}J_n(\zeta_{nm}\rho) + \frac{1}{Y_n(\zeta_{nm}\rho_1)}Y_n(\zeta_{nm}\rho). \tag{20}$$

so that eigenfunctions are given (analogously to the disc case, and before normalization) via $\varphi^{(1,2)}_{nm}(\rho,\theta) = f_{nm}(\rho)\begin{Bmatrix}\cos(n\theta)\\ \sin(n\theta)\end{Bmatrix}$. While the functional form (20) of the eigenfunctions is clearly known, the corresponding annular eigenvalues $\lambda_{nm} = \zeta^2_{nm}$ are required for the basis to be fully determined. We solve for the eigenvalues using a Newton iteration on the eigenvalue equation, with the method bootstrapped using an approximate eigenvalue obtained using the `chebfun` system [23] (whose values, at least for larger eigenvalues fail to provide adequate accuracy but are still highly useful to start a Newton iteration).

B Derivation of Padé approximations

Let f have the $(2n-1)$-th order Taylor expansion

$$f(X) = a_0 + a_1X \ldots + a_{2n-1}X^{2n-1} + o(X^{2n-1})$$

about $X = 0$. In particular, we have $a_0 = 1$ and $a_{k+1} = a_k(2k+r)/(2k+2)$ for $f(X) = (1-X)^{-r/2}$. The coefficients of the polynomials

$$P_{n-1}(X) = p_0 + p_1X \ldots + p_{n-1}X^{n-1}, \qquad Q_n(X) = 1 + q_1X \ldots + q_nX^n,$$

such that $\Pi_n[f] = P_{n-1}/Q_n$ (with the adopted normalization $q_0 = 1$ ensuring uniqueness of P_{n-1}, Q_n) are found from the linear relations

$$\begin{aligned} &\text{(a)}\quad a_{n+k} + a_{n+k-1}q_1 + \ldots + a_kq_n = 0 \qquad && (0\leq k\leq n-1),\\ &\text{(b)}\quad p_k = a_0q_k + a_1q_{k-1}\ldots + a_kq_0 && (0\leq k\leq n-1)\end{aligned} \tag{21}$$

where $q_1, \ldots q_n$ solve the n linear equations (a) and $p_0, \ldots, p_{n-1}$ are then given explicitly by relations (b). Numerical experiments for $f(X) = (1-X)^{-1/2}$ indicate however that the linear system (21a) becomes ill-conditioned for n larger than about 10. We therefore solved (21) using symbolic computation.

Declarations

- Ethical Approval and Consent to participate: Not Applicable
- Consent for publication: Not applicable.
- Human and Animal Ethics: Not applicable.
- Availability of supporting data: Not applicable.
- Competing interests: None
- Funding: We acknowledge support from NSF under grant DMS-2012424.
- Authors' contributions: All authors designed research and wrote the manuscript. M.B. developed the formulation and T.A. implemented all the algorithms and compiled the results.
- Acknowledgments: This research was supported in part through computational resources and services provided by the Advanced Research Computing (ARC) at the University of Michigan.

References

[1] Z. Lin, J.-L. Thiffeault, and C. R. Doering. "Optimal stirring strategies for passive scalar mixing". In: *Journal of Fluid Mechanics* 675 (2011), 465–476.

[2] E. Lunasin, Z. Lin, A. Novikov, A. Mazzucato, and C. R. Doering. "Optimal mixing and optimal stirring for fixed energy, fixed power, or fixed palenstrophy flows". In: *Journal of mathematical physics* 53.11 (2012), p. 115611.

[3] J.-L. Thiffeault. "Using multiscale norms to quantify mixing and transport". In: *Nonlinearity* 25.2 (2012), R1.

[4] G. Mathew, I. Mezić, and L. Petzold. "A multiscale measure for mixing". In: *Physica D: Nonlinear Phenomena* 211.1-2 (2005), pp. 23–46.

[5] M. F. Eggl and P. J. Schmid. "Mixing enhancement in binary fluids using optimised stirring strategies". In: *Journal of Fluid Mechanics* 889 (2020), A24.

[6] M. Darbas, E. Darrigrand, and Y. Lafranche. "Combining analytic preconditioner and Fast Multipole Method for the 3D Helmholtz equation". In: *J. Comput. Phys.* 236 (2013), pp. 289–316.

[7] A. Bonito and J. E. Pasciak. "Numerical approximation of fractional powers of elliptic operators". In: *Mathematics of Computation* 84 (2015), pp. 2083–2110.

[8] B. Duan, R. D. Lazarov, and J. E. Pasciak. "Numerical approximation of fractional powers of elliptic operators." In: *IMA Journal of Numerical Analysis* 40 (2020), pp. 1746–1771.

[9] A. Barnett and A. Hassell. "Fast Computation of High-Frequency Dirichlet Eigenmodes via Spectral Flow of the Interior Neumann-to-Dirichlet Map". In: *Communications on Pure and Applied Mathematics* 67.3 (2014), pp. 351–407.

[10] A. Gholami, D. Malhotra, H. Sundar, and G. Biros. "FFT, FMM, or multigrid? A comparative study of state-of-the-art Poisson solvers for uniform and nonuniform grids in the unit cube". In: *SIAM Journal on Scientific Computing* 38.3 (2016), pp. C280–C306.

[11] W. McLean. *Strongly elliptic systems and boundary integral equations*. Cambridge, 2000.

[12] J. L. Lions and E. Magenes. *Non-homogeneous boundary value problems and applications (volume 1)*. Springer, 1972.

[13] C. Brezinski. *Padé-type approximation and general orthogonal polynomials*. Vol. 50. Springer, 1980.

[14] G. A. Baker and P. Graves-Morris. *Padé approximants (second edition)*. Cambridge University Press, 1996.

[15] Clawpack Development Team. *Clawpack software*. Version 5.7.1. 2020. DOI: https://doi.org/10.5281/zenodo.4025432. URL: http://www.clawpack.org.

[16] K. T. Mandli, A. J. Ahmadia, M. Berger, D. Calhoun, D. L. George, Y. Hadjimichael, D. I. Ketcheson, G. I. Lemoine, and R. J. LeVeque. "Clawpack: building an open source ecosystem for solving hyperbolic PDEs". In: *PeerJ Computer Science* 2 (2016), e68. DOI: 10.7717/peerj-cs.68.

[17] R. J. LeVeque. *Finite Volume Methods for Hyperbolic Problems*. Cambridge University Press, 2002. URL: http://www.clawpack.org/book.html.

[18] M. Schlottke-Lakemper, G. J. Gassner, H. Ranocha, A. R. Winters, and J. Chan. *Trixi.jl: Adaptive high-order numerical simulations of hyperbolic PDEs in Julia*. https://github.com/trixi-framework/Trixi.jl. Sept. 2021. DOI: 10.5281/zenodo.3996439.

[19] R. Kress. *Linear integral equations*. Vol. 82. Springer, 1989.

[20] A. Barnett, B. Wu, and S. Veerapaneni. "Spectrally accurate quadratures for evaluation of layer potentials close to the boundary for the 2D Stokes and Laplace equations". In: *SIAM Journal on Scientific Computing* 37.4 (2015), B519–B542.

[21] T. G. Anderson, H. Zhu, and S. Veerapaneni. "A fast, high-order scheme for evaluating volume potentials on complex 2D geometries via area-to-line integral conversion and domain mappings". In: *arXiv preprint arXiv:2203.05933* (2022).

[22] G. C. Hsiao and W. L. Wendland. *Boundary integral equations*. Springer, 2008.

[23] T. A Driscoll, N. Hale, and L. N. Trefethen. *Chebfun Guide*. Pafnuty Publications, 2014. URL: http://www.chebfun.org/docs/guide/.